

See discussions, stats, and author profiles for this publication at: <https://www.researchgate.net/publication/225292613>

Conformational and Synthon Polymorphism in Furosemide (Lasix)

ARTICLE *in* CRYSTAL GROWTH & DESIGN · APRIL 2010

Impact Factor: 4.89 · DOI: 10.1021/cg100098z

CITATIONS

52

READS

96

4 AUTHORS:



Nanubolu Jagadeesh Babu

University of Nottingham

40 PUBLICATIONS 814 CITATIONS

[SEE PROFILE](#)



Suryanarayan Cherukuvada

Indian Institute of Science

20 PUBLICATIONS 244 CITATIONS

[SEE PROFILE](#)



Ranjit Thakuria

Gauhati University

21 PUBLICATIONS 320 CITATIONS

[SEE PROFILE](#)



Ashwini Nangia

University of Hyderabad

273 PUBLICATIONS 7,109 CITATIONS

[SEE PROFILE](#)

Conformational and Synthon Polymorphism in Furosemide (Lasix)

N. Jagadeesh Babu, Suryanarayana Cherukuvada, Ranjit Thakuria, and Ashwini Nangia*

School of Chemistry, University of Hyderabad, Prof. C. R. Rao Road, Gachibowli, Central University P.O., Hyderabad 500 046, India

Received January 22, 2010; Revised Manuscript Received March 2, 2010

ABSTRACT: Two polymorphs of the well-known diuretic drug Lasix, generic name furosemide, are characterized by single crystal X-ray diffraction to give a trimorphic cluster of polymorphs: known form 1 in $P\bar{1}$ space group, and novel forms 2 and 3 in $P2_1/n$ and $\bar{P}1$ space groups. The conformationally flexible molecule 4-chloro-2-[(2-furanylmethyl)amino]-5-sulfamoylbenzoic acid has variable torsions at the sulfonamide and furyl ring portions in conformers which lie in a 6 kcal mol⁻¹ energy window. A conformer surface map was calculated to show that the two conformations in crystal form 1 are ~4.5 kcal mol⁻¹ less stable than conformers present in forms 2 and 3 (0.7, 0.0 kcal mol⁻¹). The stabilization of molecular conformations is analyzed in terms of attractive intramolecular N–H···Cl hydrogen bonds and minimization of repulsive S=O···Cl interactions. Phase stability relationships confirm the thermodynamic nature of form 1 in grinding and slurry experiments by X-ray powder diffraction and infrared spectroscopy. Despite the large difference in molecular conformer energies, crystal lattice energies of polymorphs 1–3 are very close (-41.65, -41.78, -41.53 kcal mol⁻¹). These results show that the thermodynamic stability of polymorph 1 of furosemide concluded in crystallization experiments is not possible to predict through computations. Moreover, the presence of metastable conformers in the stable crystal structure reemphasizes that there is no substitute for experimental validation in polymorphic systems. The greater stability of polymorph 1 is ascribed to its more efficient crystal packing, higher density, and the presence of $R_4^2(8)$ sulfonamide N–H···O dimer synthon. Because of the differences in torsion angles and hydrogen bonding in polymorphs 1–3, they are more appropriately classified as conformational and synthon polymorphs.

Introduction

Furosemide, or frusemide, an anthranilic acid derivative having the chemical name 4-chloro-2-[(2-furanylmethyl)amino]-5-sulfamoylbenzoic acid, is marketed under the brand name Lasix.¹ The name Lasix is derived from lasts six (hours), referring to its duration of action which starts 30–60 min after oral administration of the drug. This loop diuretic drug acts on the ascending loop of Henle in the kidney to allow the removal of unneeded water and salt from the body into the urine. However, furosemide is practically insoluble in water (solubility 0.006 mg mL⁻¹). An enhanced solubility of furosemide is particularly important because its bioavailability is related to in vivo dissolution profile. Its low solubility is ascribed to strong intra- and intermolecular hydrogen bonds in the crystal structure which disfavor ready solvation/hydration of the drug. In general, physicochemical and pharmacokinetic properties of drugs, such as stability, compressibility, filterability, morphology, dissolution profile, bioavailability, tabletting, etc., can be modified by appropriate solid-state form selection,² for example, polymorph,³ hydrate, solvate, salt, or cocrystal.⁴ Three polymorphs and two solvates of furosemide have been characterized⁵ by X-ray powder diffraction (XRPD), solid-state NMR, thermal analysis (DSC, TGA), FT-IR spectroscopy, terahertz spectroscopy and hot stage microscopy (HSM), among other analytical techniques. However, single crystal X-ray diffraction on polymorphs of furosemide is scarce, despite the commercial importance of this drug. Two triclinic crystal structures⁶ of furosemide (Table 1) are reported in the Cambridge Structural Database (CSD ver. 5.30, September 2009 update).⁷ Although it was

suspected for some time that the two crystal structures are polymorphs of furosemide, careful X-ray data analysis showed that it is actually a case of pseudosymmetry leading to doubling of the unit cell, with an increase in Z' from 1 to 2. Upon repeating the experiments, Hursthouse⁸ and co-workers found that crystallization of furosemide from methanol produced small crystals that grow around the sides of the flask, while larger specimens grew on the floor of the flask. The small crystals correspond to the smaller unit cell and the larger crystals from another region of the flask gave a doubled unit cell. The larger structure having doubled a -axis has two independent molecules in the asymmetric unit that differ only in the orientation of the furan ring, whereas the small cell structure has disordered furan ring orientations. A comparison of reduced cell parameters and XRPD line profile confirmed that the two crystal structures are indeed one and the same. These experiments were repeated in our laboratory with identical results. The modulated structures in the triclinic space group $P\bar{1}$ ($Z' = 1, 2$) will be referred to as furosemide form 1. We report herein X-ray crystal structures of two new polymorphs of furosemide, forms 2 and 3, along with XRPD, FT-IR, FT-NIR, FT-Raman spectra, DSC thermograms, and phase transitions between forms 1 and 2.

Results

The chemical diagram of furosemide (Figure 1) gives an indication of the molecule's ability to exhibit conformational polymorphism.⁹ The rigid portion of the molecule is the anthranilic acid moiety, and the conformationally flexible portions are the sulfonamide group and the furan ring. An intramolecular N–H···O hydrogen bond renders rigidity to the anthranilic acid moiety; consequently, rotation about the

*To whom correspondence should be addressed. E-mail: ashwini.nangia@gmail.com.

Table 1. Unit Cell Parameters of Furosemide Form 1 Crystal Structures in the CSD and Measurements in This Study

	FURSEM01		FURSEM02		form 1 data recollected in this study ^a	
	as reported	reduced cell	as reported	reduced cell		
<i>a</i> /Å	10.467(12)	9.584	5.234(3)	5.234	5.2336(8)	9.590(5)
<i>b</i> /Å	15.801(15)	10.467	8.751(6)	8.751	8.7632(13)	10.454(5)
<i>c</i> /Å	9.584(10)	15.725	15.948(15)	14.982	14.987(2)	15.701(8)
$\alpha/^\circ$	71.87	93.47	103.68(12)	77.43	78.097(3)	93.505(9)
$\beta/^\circ$	115.04	107.27	69.94(9)	89.10	89.130(3)	107.291(8)
$\gamma/^\circ$	108.48	115.04	95.59(12)	84.41	82.330(3)	114.980(8)
<i>V</i> /Å ³	1332.84	1332.84	666.57	666.57	666.50(7)	1330.3(11)
<i>Z'</i>	2		1		1	2
3D coordinates	yes		yes		yes	yes
<i>R</i> -factor	0.068		0.11		0.093	0.071
furan ring	ordered		disordered		disordered	ordered
cell size	big		small		small	big
<i>T</i> /K	298		298		298	298
year	1978 (ref 6b)		1983 (ref 6c)		2008	2008

^a Big unit cell data was recollected at 100 K and solved crystal structure is reported in Table 2.

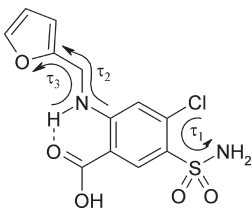


Figure 1. The three torsion parameters in furosemide: $\tau_1 = \text{C}-\text{C}-\text{S}-\text{N}$, $\tau_2 = \text{C}-\text{N}-\text{C}-\text{C}$, $\tau_3 = \text{N}-\text{C}-\text{C}-\text{O}$. The anthranilic acid moiety is locked in an intramolecular hydrogen bond.

phenyl–carboxylic acid C–C bond is difficult. Sulfonamide and furan ring torsions can result in different conformers in solution, thereby increasing the likelihood of polymorphism in the solid-state.

We repeated crystallization of furosemide to confirm the two triclinic structures of form 1 (Table 1). Two crystal morphologies, platelike (a few) and needles to block (major), were found in crystallization batches of furosemide from *n*-propanol. Data were collected on a single crystal representing each unique morphology and *hkl* reflections were viewed in the RLATT program. The small unit cell crystal structure has strong *h*-even reflections along with a few very weak *h*-odd X-ray reflections (see Figure S1 for RLATT screen shot, Supporting Information); the weak reflections were not picked up by the automated software for unit cell determination, data reduction, and structure solution. The resulting crystal structure (*a* = 5.24 Å) has one molecule in the asymmetric unit with the furan ring being disordered over two sites of equal occupancy. When *h*-odd reflections of the big unit cell data, which are now about equal in number to *h*-even reflections, were together used to solve the structure, a doubled unit cell (*a* = 10.47 Å) with two symmetry independent ordered molecules in different furan ring orientations was obtained. Crystal data of furosemide form 1 triclinic structures is reproducible.

The crystal structure of furosemide form 1 ($P\bar{1}$, $Z' = 2$, 100 K) is discussed. The two conformers are identical at the sulfonamide group (τ_1 166.0, 163.2°) but have different orientations of the furan ring, τ_2 (83.9, 61.4°) and τ_3 (68.2, 57.6°). In general, the dihedral angle is a soft geometrical parameter, and τ differences of 2–3° (even up to 5°) may be treated as similar conformers. Symmetry-independent molecules aggregate via the carboxylic acid dimer ($O4-H4 \cdots O8$: 1.68 Å, 2.672(5) Å, 179.9°; $O9-H9 \cdots O3$: 1.65 Å, 2.635(5) Å, 173.1°;

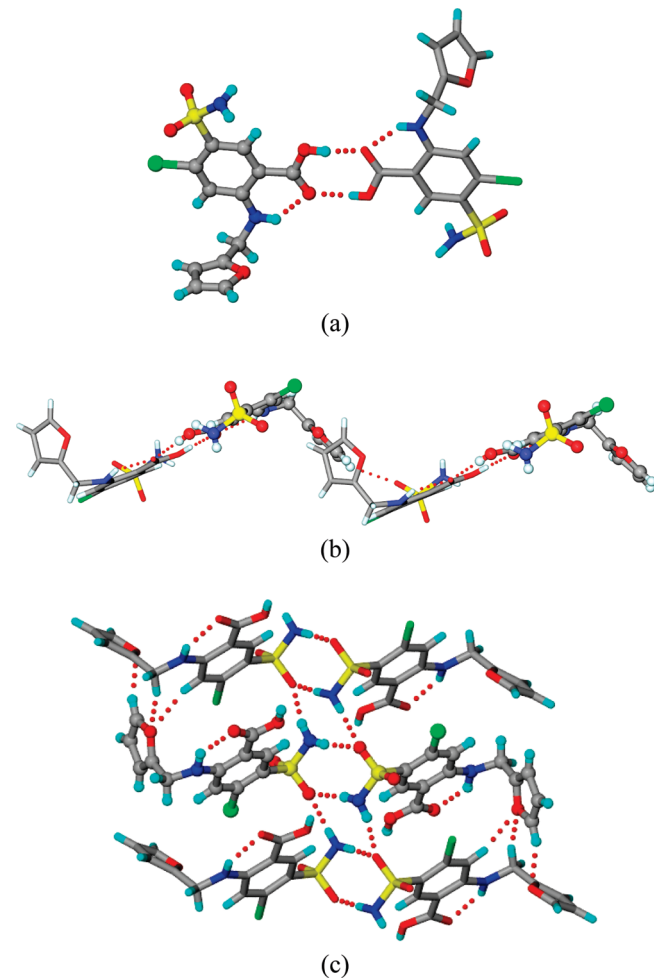


Figure 2. (a) Carboxylic acid O–H \cdots O dimer synthon between symmetry-independent molecules of furosemide ($Z' = 2$) extend to make a corrugated 2D sheet (b) in form 1. (c) Centrosymmetric sulfonamide N–H \cdots O dimers complete the 3D packing. Crystallographic unique molecules differing in the furan ring orientation are shown as ball-stick and capped-stick models.

Figure 2a), and the secondary amine N–H forms an intramolecular N–H \cdots O with the carbonyl group (N2–H2 \cdots O3: 1.91 Å, 2.744(5) Å, 137.6°; N5–H5 \cdots O8: 1.92 Å, 2.747(4) Å, 136.8°). These molecules extend via weak C–H \cdots O interactions to form a corrugated sheet structure

Table 2. Crystallographic Parameters of Polymorphs 1–3 of Furosemide

	form 1	form 2	form 3
chemical formula	C ₁₂ H ₁₁ ClN ₂ O ₅ S	C ₁₂ H ₁₁ ClN ₂ O ₅ S	C ₁₂ H ₁₁ ClN ₂ O ₅ S
formula weight	330.74	330.74	330.74
crystal system	triclinic	monoclinic	triclinic
space group	P <bar{1}< td=""><td>P2₁/n</td><td>P<bar{1}< td=""></bar{1}<></td></bar{1}<>	P2 ₁ /n	P <bar{1}< td=""></bar{1}<>
T/K	100(2)	100(2)	100(2)
a/ \AA	9.5150(9)	5.0097(5)	4.8764(7)
b/ \AA	10.4476(10)	10.1086(11)	10.4999(14)
c/ \AA	15.5826(16)	26.620(3)	13.6407(18)
$\alpha/^\circ$	92.839(2)	90	78.065(2)
$\beta/^\circ$	107.088(2)	95.396(2)	86.721(2)
$\gamma/^\circ$	116.7470(10)	90	82.589(2)
Z/Z'	4/2	4/1	2/1
V/ \AA^3	1291.9(2)	1342.1(2)	677.29
D _{calc} /g cm ⁻³	1.700	1.637	1.622
μ/mm^{-1}	0.482	0.464	0.460
reflns collected	13411	13596	7005
unique reflns	5061	2655	2631
observed reflns	3466	2101	2063
R ₁ [I > 2 σ (I)]	0.0668	0.0596	0.0562
wR ₂ [all]	0.1258	0.1249	0.1139
goodness-of-fit	1.050	1.116	1.052
diffractometer	SMART-APEX CCD	SMART-APEX CCD	SMART-APEX CCD

Table 3. Hydrogen Bonds in Crystal Structures of Furosemide^a

interaction	H ··· A/Å	D ··· A/Å	$\angle D-H \cdots A/^\circ$	symmetry code
Form 1				
O4—H4 ··· O8	1.68	2.672(5)	179.9	$-1+x, y, -1+z$
O9—H9 ··· O3	1.65	2.635(5)	173.1	$1+x, y, 1+z$
N1—H1A ··· O2	1.98	2.978(5)	170.6	$1-x, 1-y, -z$
N1—H1B ··· O7	2.28	3.099(6)	137.2	$1-x, 2-y, 1-z$
N2—H2 ··· O3	1.91	2.744(5)	137.6	^b
N3—H3A ··· O7	1.99	2.999(5)	172.2	$1-x, 2-y, 2-z$
N3—H3B ··· O2	1.99	2.926(6)	151.9	$1-x, 1-y, 1-z$
N5—H5 ··· O8	1.92	2.747(4)	136.8	^b
C3—H3 ··· O7	2.55	3.137(6)	112.8	$1-x, 2-y, 1-z$
C6—H6 ··· O10	2.32	3.381(5)	163.4	$1-x, 1-y, 1-z$
C11—H11 ··· O6	2.48	3.452(5)	148.6	x, y, z
C8—H8A ··· O10	2.60	3.611(6)	153.8	$1-x, 1-y, -z$
C8—H8B ··· O1	2.54	3.155(6)	114.7	$-1+x, y, z$
C20—H20A ··· O6	2.44	3.217(6)	127.3	$1+x, y, z$
C20—H20B ··· O1	2.50	3.312(6)	130.7	$2-x, 2-y, 1-z$
C24—H24 ··· O5	2.54	3.378(6)	132.7	$1-x, 1-y, 1-z$
Form 2				
O4—H4 ··· O3	1.65	2.640(4)	178.0	$-1-x, 2-y, -z$
N2—H2 ··· O3	1.81	2.652(4)	138.2	^b
N1—H1A ··· O1	2.17	3.113(4)	154.4	$1/2-x, -1/2+y, 1/2-z$
N1—H1B ··· O2	1.97	2.960(4)	164.1	$-1+x, y, z$
C8—H8A ··· O5	2.49	3.368(5)	136.4	$-x, 1-y, -z$
C8—H8B ··· O3	2.66	3.404(4)	125.0	$1+x, y, z$
C11—H11 ··· O2	2.77	3.594(5)	131.8	$-1/2+x, 1/2-y, -1/2+z$
Form 3				
O4—H4 ··· O3	1.67	2.644(3)	168.5	$-1-x, 1-y, 1-z$
N2—H2 ··· O3	1.86	2.670(4)	134.5	^b
N1—H1B ··· Cl1	2.66	3.252(4)	117.0	^b
N1—H1A ··· O2	2.05	3.028(4)	161.0	$1-x, -y, 1-z$
N1—H1A ··· O2	2.35	2.911(4)	113.9	$1+x, y, z$
N1—H1B ··· O1	2.37	3.178(4)	136.2	$1+x, y, z$
C3—H3 ··· O2	2.52	3.610(4)	175.3	$-x, -y, 1-z$
C8—H8A ··· O1	2.24	3.310(4)	165.9	$x, 1+y, z$

^aO—H, N—H, and C—H distances are neutron-normalized to 0.983, 1.009, and 1.083 Å. ^bIntramolecular hydrogen bond.

(C8—H8B ··· O1: 2.54 Å, 3.155(6) Å, 114.7°; C11—H11 ··· O6: 2.48 Å, 3.452(5) Å, 148.6°; C20—H20A ··· O6: 2.44 Å, 3.217(6) Å, 127.3°). Sulfonamide N—H and O atoms point up and downwards in the 2D layer (Figure 2b) to form centrosymmetric dimers using an NH donor (N1—H1A ··· O2: 1.98 Å, 2.978(5) Å, 170.6°; N3—H3A ··· O7: 1.99 Å, 2.999(5) Å, 172.2°). Such dimers are connected by N—H ··· O hydrogen

bonds via the second NH donor (N1—H1B ··· O7: 2.28 Å, 3.099(6) Å, 137.2°; N3—H3B ··· O2: 1.99 Å, 2.926(6) Å, 151.9°; Figure 2c). Crystallographic data are summarized in Table 2 and hydrogen bonds are listed in Table 3.

Form 2 crystallized in the monoclinic space group with one furosemide molecule ($Z' = 1$). When reflections were collected at 293 K, the furan ring was found to be disordered over

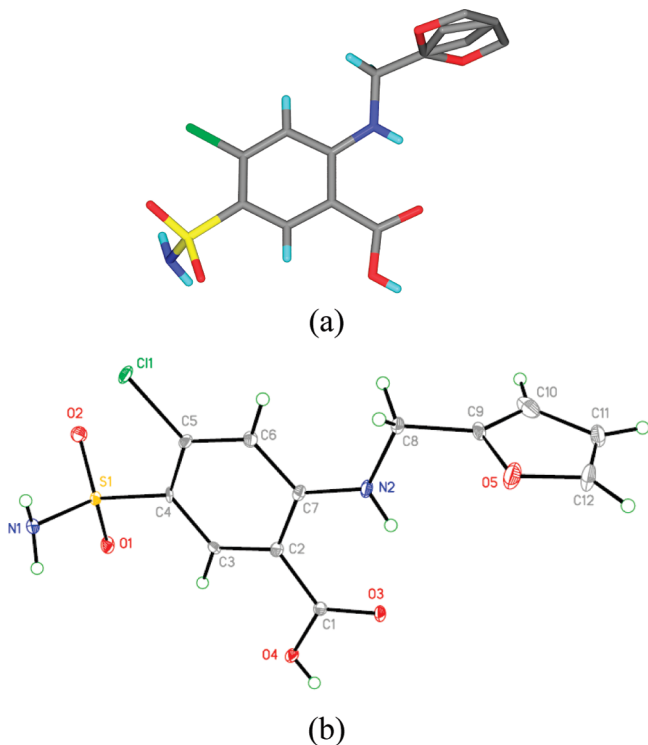


Figure 3. (a) Furosemide form 2 data collected at 293 K show the furan ring disordered over two sites with 75% and 25% site occupancy of atoms. (b) ORTEP at 50% probability of non-hydrogen atoms for reflections collected at 100 K shows a fully ordered structure.

two sites with 75% and 25% site occupancy of ring atoms. A single orientation of the furan ring was observed when reflections were collected on the same crystal at 100 K (Figure 3). The secondary amine N–H forms an intramolecular N–H···O with the carbonyl group of carboxylic acid (N2–H2···O3: 1.81 Å, 2.652(4) Å, 138.2°), similar to form 1. However, the structure is not layered, like in form 1 (and form 3, discussed next), but has a helical motif of N–H···O hydrogen bonds. Carboxylic acid dimers (O4–H4···O3: 1.65 Å, 2.640(3) Å, 178.0°) are connected to 2-fold screw-axis related molecules along the *b*-axis via parallel infinite chains of N–H···O hydrogen bonds (catemer synthon) involving one of the sulfonamide NH donors (N1–H1A···O1: 2.17 Å, 3.113(4) Å, 154.4°; Figure 4). The second sulfonamide NH donor and O acceptor form a tetramer network made up of hydrogen bonds (N1–H1B···O2: 1.97 Å, 2.960(4) Å, 164.1°). Auxiliary C–H···O interactions complete the crystal packing.

Form 3 crystallized in *P*1 space group (100 K) with one molecule of furosemide ($Z' = 1$) in the asymmetric unit. The secondary amine N–H forms an intramolecular N–H···O with the carbonyl group of carboxylic acid (N2–H2···O3: 1.86 Å, 2.670(4) Å, 134.5°). There is another intramolecular hydrogen bond of sulfonamide NH with the adjacent chlorine atom (N1–H1B···Cl1: 2.66 Å, 3.252(4) Å, 117.0°). Centrosymmetric carboxylic acid dimers (O4–H4···O3: 1.67 Å, 2.644(3) Å, 168.5°) form zigzag tapes via weak C–H···O dimer (C3–H3···O2: 2.52 Å, 3.610(4) Å, 175.3°) and such tapes make a corrugated 2D sheet through close packing of furan rings (Figure 5). The sulfonamide N–H and O atom pointing up and downward from the 2D layer to assemble the SO₂NH dimer (N1–H1A···O2: 2.05 Å, 3.028(4) Å, 161.0°).

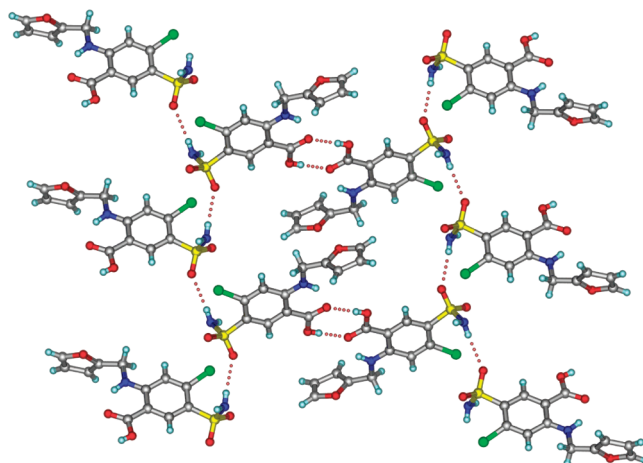


Figure 4. Sulfonamide N–H···O helices along the *b*-axis (catemer synthon) connect carboxylic acid dimers in the crystal structure of furosemide form 2.

The N–H donors and SO₂ acceptors join sulfonamide dimers such that H1 makes a bifurcated motif (N1–H1A···O2: 2.35 Å, 2.911(4) Å, 113.9°; N1–H1B···O1: 2.37 Å, 3.178(4) Å, 136.2°).

Discussion

Conformational and Synthon Polymorphs. Polymorphs may be classified into three main categories. (1) When the arrangement of rigid molecules, or of flexible molecules in the same conformation, is different in different crystal structures, they are called packing polymorphs,¹⁰ for example, trimorphs of benzamide,¹¹ or tetramorphs of carbamazepine.¹² These crystal structures are sustained by the carboxamide N–H···O dimer, but there are differences in molecular packing due to the ways in which these dimers are organized in the crystal lattice. (2) Differences in molecular conformation leading to different crystal structures is referred to as conformational polymorphism,¹³ for example, dimorphs of ritonavir,¹⁴ pentamorphs of tolfenamic acid,¹⁵ or polymorphs of ROY.¹⁶ (3) When hydrogen bonding, or supramolecular synthon, is different in different crystal structures of the same compound, it is termed synthon polymorphism,¹⁷ for example, differences in carboxylic acid, carboxamide or sulfonamide motifs (acid dimer vs catemer in oxalic acid and tetrolic acid),¹⁸ and temozolomide¹⁹ or sulfathiazole²⁰ (different N–H···O and N–H···N hydrogen bond motifs). Of course, these classifications can be somewhat subjective because there is a certain degree of overlap possible between them and more than one can coexist in a given system, for example, conformational and synthon polymorphism or synthon and packing polymorphism. It is important to recall that despite significant hydrogen bonding, conformation, packing, and unit cell differences between alternative crystal structures of polymorphs, their energy difference is generally small, typically 0.5–3.0 kcal mol^{−1} and rarely exceeds 5 kcal mol^{−1}. We will use and justify the terms conformational and synthon polymorphs for furosemide.

An intramolecular N–H···O hydrogen bond and carboxylic acid dimer are present in all polymorphic structures of furosemide. However, hydrogen bonding of the sulfonamide group is different leading to variation in synthons. The sulfonamide group is similar to carboxamide except that it

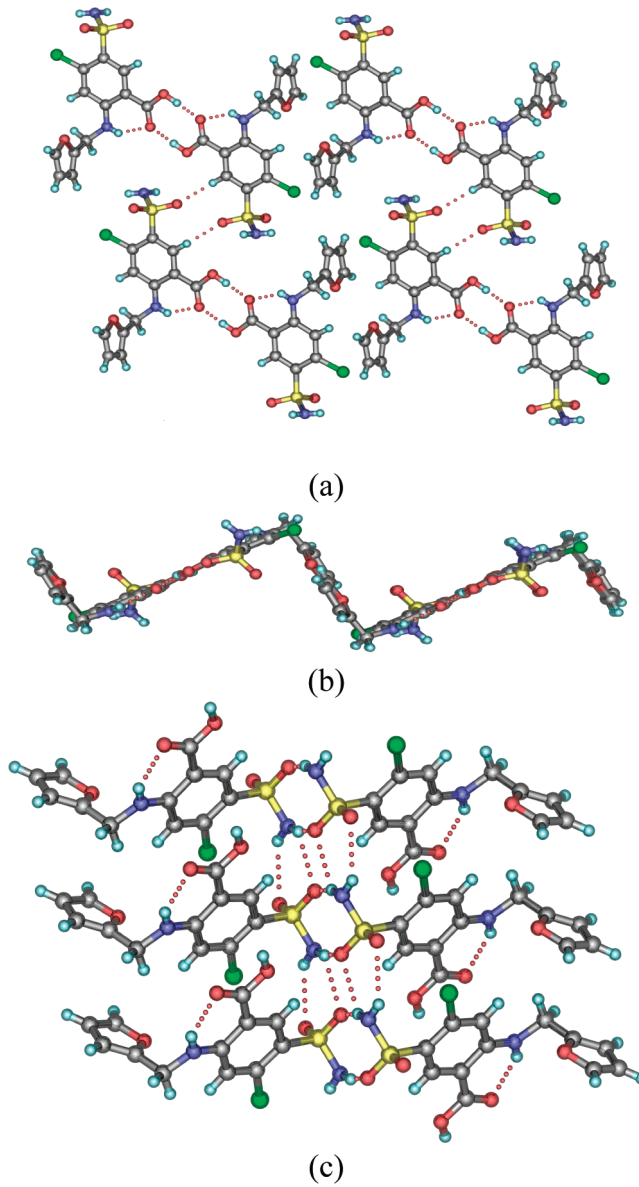


Figure 5. Arrangement of furosemide molecules in a corrugated 2D sheet sustained by $\text{O}-\text{H}\cdots\text{O}$ and $\text{N}-\text{H}\cdots\text{O}$ hydrogen bonds (a and b) in form 3. (c) Hydrogen bonding of the SO_2NH_2 group as a dimer along with $\text{N}-\text{H}\cdots\text{O}$ cross-links.

has an extra $\text{S}=\text{O}$ acceptor. When a single O acceptor participates in bifurcated hydrogen bonding, the linear tape of SO_2NH_2 in form 1 is similar to the CONH_2 tape. The graph set notation²¹ of $\text{N}-\text{H}\cdots\text{O}$ hydrogen bonds in form 1 are $R_2^2(8)$ dimer and $R_4^2(8)$ ring (Figure 6). When the SO_2 group twists outward from the linear tape, one of the bonds is broken to give a $C(4)$ $\text{N}-\text{H}\cdots\text{O}$ catemer and larger motif of $R_4^4(14)$ ring in form 2. On the other hand, if the SO_2 group moves inward so that the sulfonamide group lies parallel to the tape growth direction, additional $\text{N}-\text{H}\cdots\text{O}$ bonds are possible between the $R_2^2(8)$ dimers in form 3 as $R_2^2(6)$ rings. In effect, form 1 synthon transforms to a tighter network of H bonds in form 3, but H bonds are fewer in form 2. For comparison, 6 molecules of furosemide in Figure 6 make a dense network of 14 hydrogen bonds in form 3 (skewed dimer synthon) compared to 7 hydrogen bonds in form 2 (catemer synthon), while there are 10 hydrogen bonds in form 1 (dimer synthon). Out of 65 primary sulfonamides in

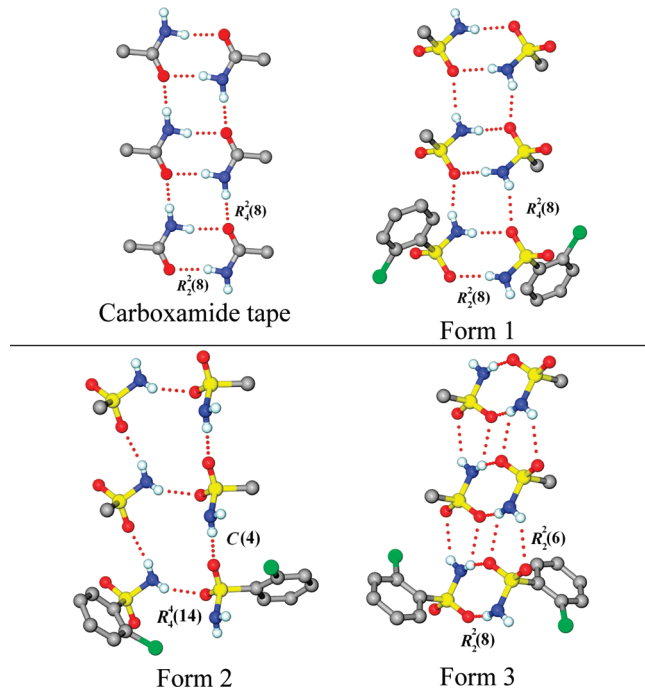


Figure 6. Synthon polymorphs of furosemide: $R_2^2(8)$ $\text{N}-\text{H}\cdots\text{O}$ dimer and $R_4^2(8)$ motif in form 1 (similar to carboxamide), $C(4)$ catemer and $R_4^4(14)$ tetramer motif in form 2, $R_2^2(8)$ $\text{N}-\text{H}\cdots\text{O}$ motif and $R_2^2(6)$ rings in skewed dimer form 3. Anthranilic acid moiety is not shown for clarity.

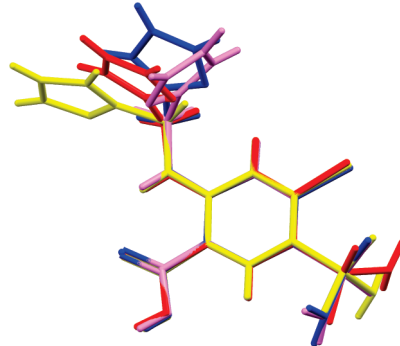


Figure 7. Overlay of four conformations in furosemide crystal structures. Form 1 conformers (magenta and blue) have similar τ_1 but different τ_2 and τ_3 values, whereas all three torsion angles are different in form 2 and 3 conformers (yellow and red). See Figure 1 for τ definition.

the CSD, 24 crystal structures contain the $R_2^2(8)$ sulfonamide $\text{N}-\text{H}\cdots\text{O}$ dimer synthon, whereas $R_2^2(6)$ and $R_4^4(14)$ ring motifs are rare (1, 0 hits). Surprisingly, even though the carboxamide tape is a common motif, the similar sulfonamide tape present in form 1 is as such limited to furosemide only (FURSEM03).

The molecular conformations too are different in polymorphs: the NH_2 group of sulfonamide is anti to the $\text{Cl}-\text{Ph}$ group in form 1, orthogonal to the aromatic plane in form 2, and syn in form 3. Different orientations of the furyl ring are observed in crystal structures. An overlay diagram of the four conformers in three polymorphs shows that the two conformers of form 1 differ only in the furyl ring portion (τ_2 and τ_3) but not the sulfonamide moiety (τ_1), whereas conformations in form 2 and 3 differ in both portions of the molecule (Figure 7). The anthranilic acid portion of the

molecule is locked by an intramolecular N–H···O hydrogen bond that constrains conformational flexibility. The energy profile of SO_2NH_2 group orientations on N-methylchloranthranilic acid is plotted in Figure 8. There is a metastable shallow minimum of conformers in which the NH_2 group (of sulfonamide) is antiperiplanar to the adjacent Cl (of chlorophenyl) centered at $\tau_1 = 180 \pm 30^\circ$, which contains form 1 conformer too. The more stable conformations of form 2 and 3 lie in a deep well minimum centered at $60 \pm 15^\circ$. The truncation of the $\text{N}-\text{CH}_2$ -furyl group by N-methyl to reduce the number of possible conformers and computation time is a valid approximation to estimate furosemide conformation energies as a function of sulfonamide group rotation. The conformation energy calculated for the molecule in form 1A, form 1B, form 2, and form 3 (4.45, 4.55, 0.71, and 0.00 kcal mol⁻¹, Table 4) matches that estimated from the energy vs torsion profile of Figure 8 (4.25, 4.53, 0.97, and 0.00 kcal mol⁻¹, the lowest energy conformer

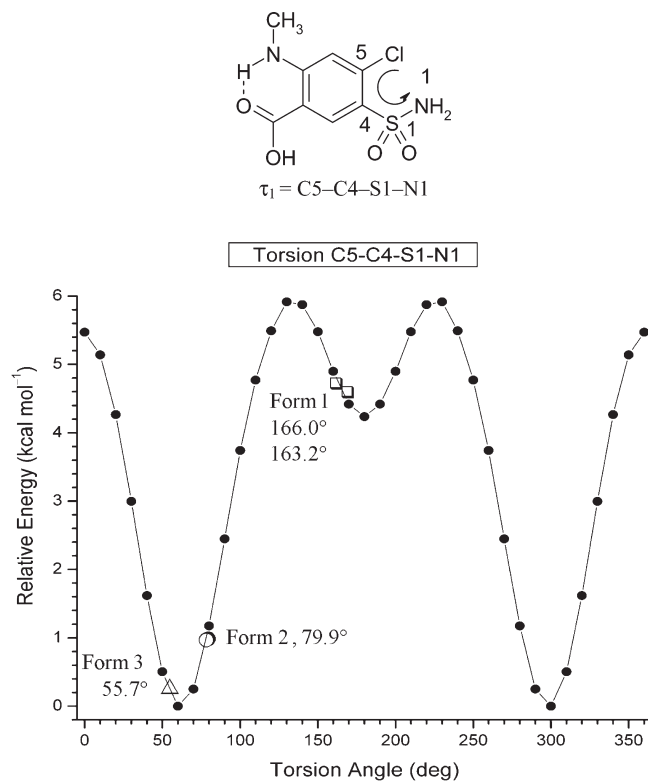


Figure 8. Furosemide is truncated to its N-methyl derivative at the $\text{N}-\text{CH}_2$ -furyl portion. Conformer energies are plotted for every 10° change in sulfonamide torsion angle τ_1 between 0 and 180° . The energy profile is symmetric about $\tau_1 = 180^\circ$. The four conformers of furosemide are placed on the plot according to their τ_1 value listed in Table 4: form 1 (□), form 2 (○), and form 3 (△).

Table 4. Conformer Torsion Angle^a (from X-ray Structure), Computed Energy^b (Gaussian 03, DFT, B3LYP/6-31G (d,p)), and Crystal Lattice Energy (Cerius², COMPASS Force Field) of Furosemide

conformer	τ_1 /°	τ_2 /°	τ_3 /°	conformer energy/kcal mol ⁻¹	conformer energy ^c /kcal mol ⁻¹	dipole moment/Debye	lattice energy/kcal mol ⁻¹
form 1A	166.0	83.9	68.2	4.447	4.25	7.095	-41.65
form 1B	163.2	61.4	57.6	4.551	4.53	6.402	
form 2	79.9	166.4	78.2	0.713	0.97	6.712	-41.78
form 3	55.7	91.3	59.9	0	0	6.867	-41.53

^a Absolute value of torsion angles is quoted. ^b The lowest energy conformer is arbitrarily set to 0. ^c Estimated from the τ_1 torsion angle of energy profile in Figure 8.

is set to 0.00). The difference in energy between conformers A and B of form I having different furyl group orientations is ~ 0.1 kcal mol⁻¹ (Table 4), which is the upper limit for furyl ring conformer energy differences when the sulfonamide moiety was frozen in Gaussian calculations.²²

The spread of conformer energies in a 6 kcal mol⁻¹ window as a function of τ_1 angle rotation is understood by accounting for the attractive and repulsive forces in the molecule. The van der Waals radius sum for Cl···O interaction is 3.27 Å (1.75 + 1.52), for Cl···N is 3.30 Å (1.75 + 1.55), and for N–H···Cl hydrogen bond is 2.84 Å (1.09 + 1.75). Two factors are decisive to determine the conformer energy as the SO_2NH_2 group rotates about the C–S bond: attractive N–H···Cl hydrogen bond and repulsive Cl···O/N interactions at shorter than vdW sum distance. The values of these interactions for the N-Me analog calculated at 10° increments are given in Table 5. They are styled as red (for repulsive short contacts), magenta (for energy neutral contacts longer than vdW sum), and green (for stabilizing hydrogen bonds). In $\tau_1 = 0$ – 30° range, the energy of conformers is high because of repulsive Cl···N contacts (< 3.30 Å, red

Table 5. Attractive (green), Repulsive (red), and Energy Neutral (magenta) Interactions and Conformer Energy of N-Me Molecule Shown in Figure 8 as a Function of Torsion Angle

Torsion τ_1 /°	Cl···N / Å	Cl···O3 / Å	Cl···O9 / Å	Conformer energy / kcal mol ⁻¹
0	3.102	4.462	4.464	5.473
10	3.110	4.297	4.595	5.139
20	3.133	4.097	4.690	4.265
30	3.170	3.873	4.745	2.997
40	3.220 2.56, 122.7°	3.645	4.764	1.620
50	3.284 2.61, 124.1°	3.456	4.762	0.505
60	3.375 2.71, 123.4°	3.309	4.759	0
70	3.505 2.87, 121.2°	3.192	4.760	0.251
80	3.690	3.106	4.772	1.176
90	3.927	3.036	4.779	2.447
100	4.179	2.985	4.757	3.742
110	4.407	2.959	4.690	4.772
120	4.582	2.951	4.584	5.493
130	4.719	2.958	4.434	5.917
140	4.814	2.976	4.239	5.875
150	4.869	3.028	4.006	5.478
160	4.889	3.109	3.770	4.899
170	4.890	3.220	3.551	4.420
180	4.889	3.368	3.367	4.237

^a N–H···Cl hydrogen bond geometry is given for those conformers only in which the geometry is short and linear ($d < 2.9$ Å, $\theta > 120^\circ$).

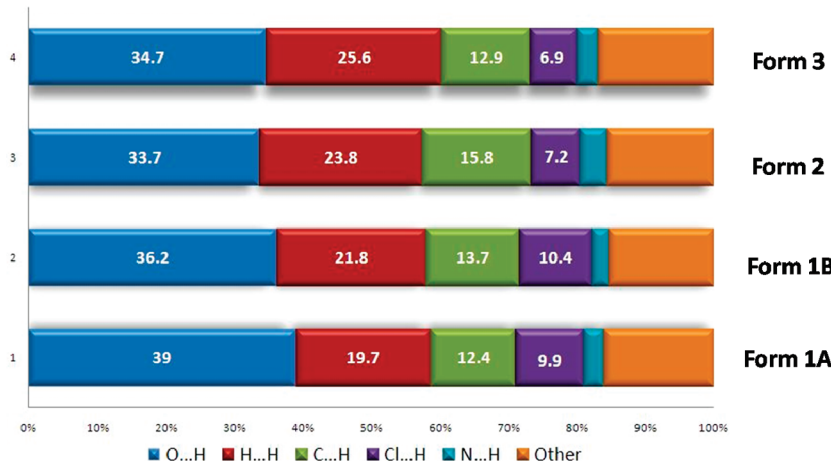


Figure 9. Percentage contributions to the Hirshfeld surface for different intermolecular interactions in furosemide forms 1, 2, and 3.

zone) and the absence of $\text{N}-\text{H}\cdots\text{Cl}$ hydrogen bonds in a bent geometry. There are $\text{Cl}\cdots\text{O}$ contacts but they are long and neither strongly attractive nor repulsive (magenta zone) in nature. Between 40 and 70° torsion, the NH donor is oriented toward the Cl acceptor making intramolecular $\text{N}-\text{H}\cdots\text{Cl}$ hydrogen bonds (green zone) and the $\text{Cl}\cdots\text{N}$ distance is $\sim\text{vdW}$ sum. For these reasons, the global energy minimum for furosemide molecule is centered at $\tau_1 = 60^\circ$. As the torsion angle increases beyond 70° , energy of the conformer rises because one of the oxygen atoms (O_3) starts moving closer to the chlorine atom and into the repulsive region. The energy peaks around $120\text{--}130^\circ$ due to this repulsive contact, but the geometry relaxes with further increase in angle and oxygen (O_3) moves away from chlorine at $\sim 160^\circ$. This gives a second dip in the conformer energy, or the metastable minimum of conformers centered at $\tau_1 = 175^\circ$.

The occurrence of metastable conformer(s) in the stable form 1 crystal structure of furosemide is surprising because many similar molecules in the CSD contain the stable molecular conformation. Out of 17 ortho-chlorophenyl primary sulfonamides in the CSD, only one crystal structure lies in the metastable minimum range, and that is furosemide form 1 (FURSEM03 164, 166°) (see Table S1, Supporting Information). The occurrence of a metastable conformer(s) in the stable polymorph is not unprecedented in conformational polymorphs; as a matter of fact intramolecular and intermolecular energy compensation is the more frequent norm.¹³ The fact that forms 1, 2, and 3 of furosemide have different molecular conformations associated with different hydrogen bond synthons justifies the term conformational and synthon polymorphs for furosemide. In a sense all polymorphs arise from a difference in molecular packing, and so referring to them as packing polymorphs is a gross classification that does not manifest structural details. An advantage with using exact definitions such as packing, conformational or synthon polymorphs is that the nature of difference between alternative crystal structures is immediately revealed for classification and quantification.

Hirshfeld surface²³ is a useful tool to quantify the contribution to crystal packing from various types of intermolecular interactions. For the understanding of crystal packing in the context of crystal design and crystal engineering, short intermolecular contacts are deemed to be important. Thus, for the analysis of furosemide polymorphs and to compare their similarities and differences Hirshfeld surface is

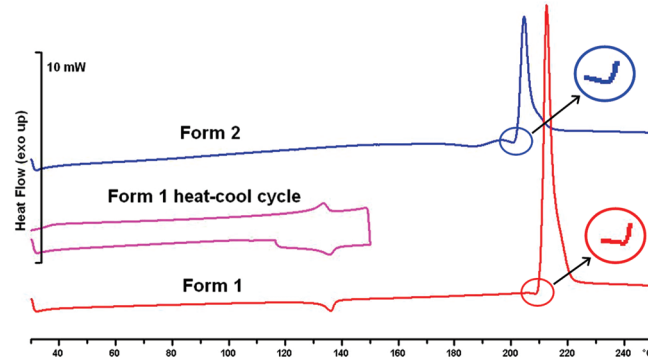


Figure 10. DSC of furosemide. Heat-cool cycle of form 1 indicates reversible phase transition at $132\text{--}137\text{ }^\circ\text{C}$. A very small melting endotherm at $207\text{ }^\circ\text{C}$ (shown in inset) is followed by a large exotherm between 210 and $217\text{ }^\circ\text{C}$ due to decomposition of furosemide (see Scheme S1 for degradation reaction). The endotherm and exotherm in form 2 occur at $198\text{ }^\circ\text{C}$ and $202\text{--}208\text{ }^\circ\text{C}$.

a useful tool. The relative contributions of the major intermolecular contacts are shown in Figure 9. Form 1 has the highest exposure to $\text{O}\cdots\text{H}$ interactions due to sulfonamide dimer synthon, whereas form 2 has the lowest $\text{O}\cdots\text{H}$ contribution to crystal lattice stabilization. All three polymorphs have a carboxylic acid dimer of $\text{O}-\text{H}\cdots\text{O}$ hydrogen bonds, but the $\text{Cl}\cdots\text{H}$ contribution is more in form 1 compared to forms 2 and 3.

Phase Stability of Forms 1–3. Crystal lattice energies of forms 1–3 computed using the COMPASS force field are too close (form 1 –41.65, form 2 –41.78, and form 3 –41.53 kcal mol⁻¹) to infer stability relationships. Several crystallization experiments yielded concomitant mixture of forms 1 + 2 from MeOH, forms 1 + 3 from AcOH and *n*-propanol, suggesting that all these crystal structures are nearly equienergetic. Energy differences between concomitant polymorphs are generally very small, typically $< 1\text{ kcal mol}^{-1}$. The stable polymorph was concluded by comparing crystal density, packing fraction, and phase transition from grinding and slurry-crystallization experiments. The higher crystal density and packing fraction (polymorphs 1, 2, 3: $D_c = 1.70, 1.64,$ and 1.62 g cm^{-3} ; $C_k = 74.0, 71.1,$ and 70.6%) indicate that form 1 is the most stable followed by forms 2 and 3 of progressively lower stability.²⁴ It is difficult to conclude about polymorph stability by melting point

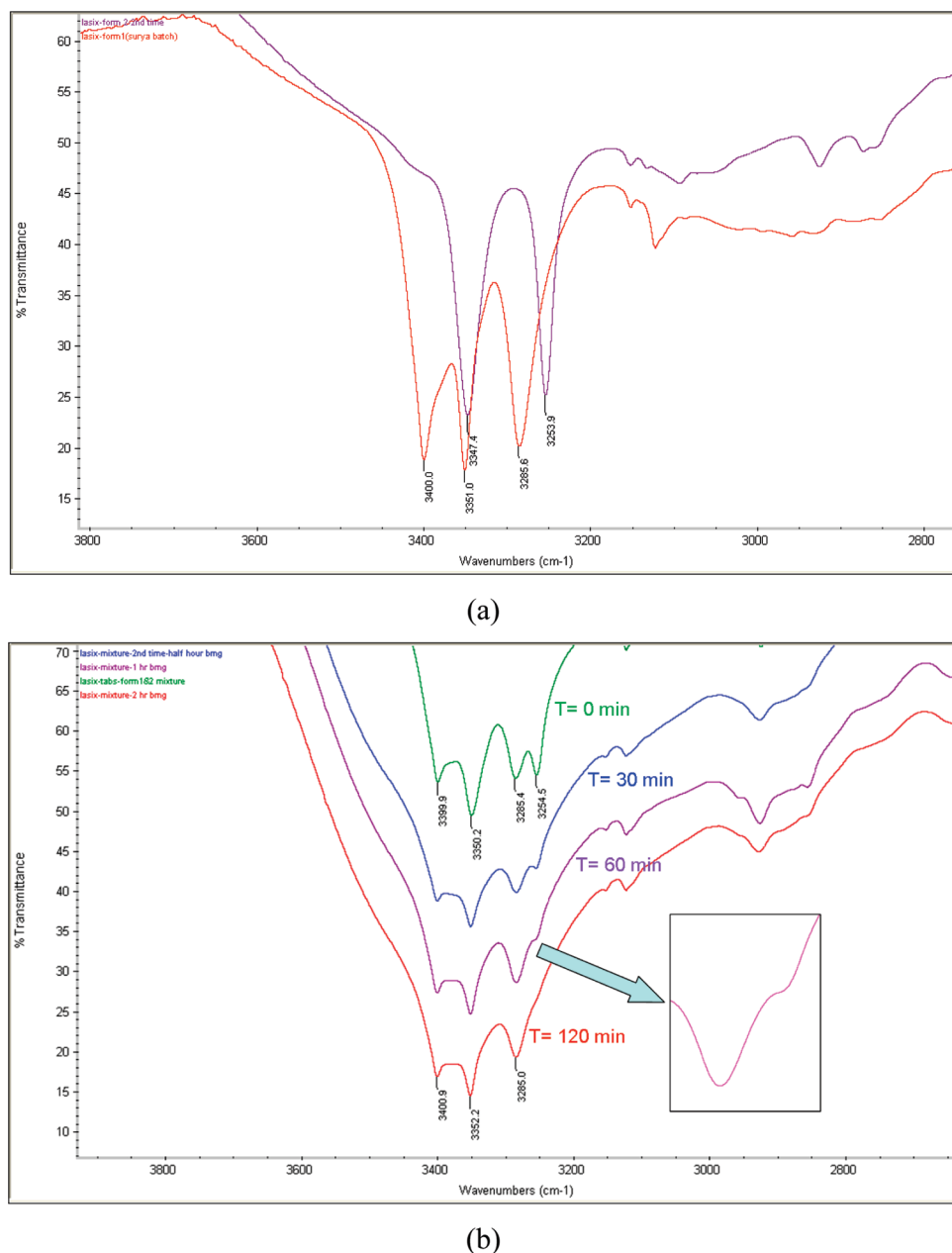


Figure 11. (a) IR spectrum (KBr, cm^{-1}) of furosemide polymorphs in pure state. Form 1 (red) shows three sharp resonances at 3400.0 cm^{-1} (asymmetric sulfonamide NH stretch), 3351.0 cm^{-1} (secondary amine NH), and 3285.6 cm^{-1} (symmetric sulfonamide NH). Form 2 (magenta) shows two diagnostic peaks at 3347.4 cm^{-1} (secondary amine NH) and 3253.9 cm^{-1} (symmetric sulfonamide NH). (b) Phase changes upon grinding were monitored by IR spectroscopy. Starting from a mixture of forms 1 and 2 (green plot, peaks at 3399.9 , 3350.2 , 3285.4 , 3254.5 cm^{-1}) to blue trace (30 min), magenta (60 min) showed almost complete conversion to form 1 peaks at 3400.9 , 3352.2 , 3285.0 cm^{-1} . There is no change in the IR spectrum after 120 min confirming stability of the product phase.

because all three polymorphs transform to a high temperature phase above $130\text{ }^{\circ}\text{C}$.^{5b} The enthalpy values of phase transformation and decomposition calculated by DSC (Figure 10) are consistent with the literature values listed in Table S2, Supporting Information (form 1: endotherm of 2.56 kJ mol^{-1} at $132\text{--}137\text{ }^{\circ}\text{C}$, exotherm of 32.98 kJ mol^{-1} at $210\text{--}217\text{ }^{\circ}\text{C}$; form 2: endotherm of 1.19 kJ mol^{-1} at $181\text{--}187\text{ }^{\circ}\text{C}$; exotherm of 33.26 kJ mol^{-1} at $202\text{--}208\text{ }^{\circ}\text{C}$). The melting endotherm is very small for furosemide polymorphs (see expanded endotherm in the inset of Figure 10) because the compound decomposes at its melting temperature (Scheme S1, Supporting Information) and the exotherm heat evolution dominates the thermogram. Visualization of the three polymorphs under a hot stage microscope (see

Supporting Information, Figure S2–S4) showed melting/decomposition above $200\text{ }^{\circ}\text{C}$. However, no morphological phase change could be detected in HSM corresponding to the $132\text{--}137\text{ }^{\circ}\text{C}$ endotherm in DSC of form 1.

Forms 1 and 2 were obtained in sufficient quantity and a pure state (Figure S5, S6, Supporting Information) to carry out solid-state grinding and slurry crystallization experiments. Form 3 crystals appeared concomitantly in very small amounts along with the major product being form 1 crystals in AcOH and *n*-propanol solvents (Figure S7, S8, Supporting Information). Single crystals of form 3 are needle/platelike which show less extinction under polarized microscope for visual polymorph screening. Fingerprint match of XRPD lines indicates that X-ray crystal structures of forms 2 and 3

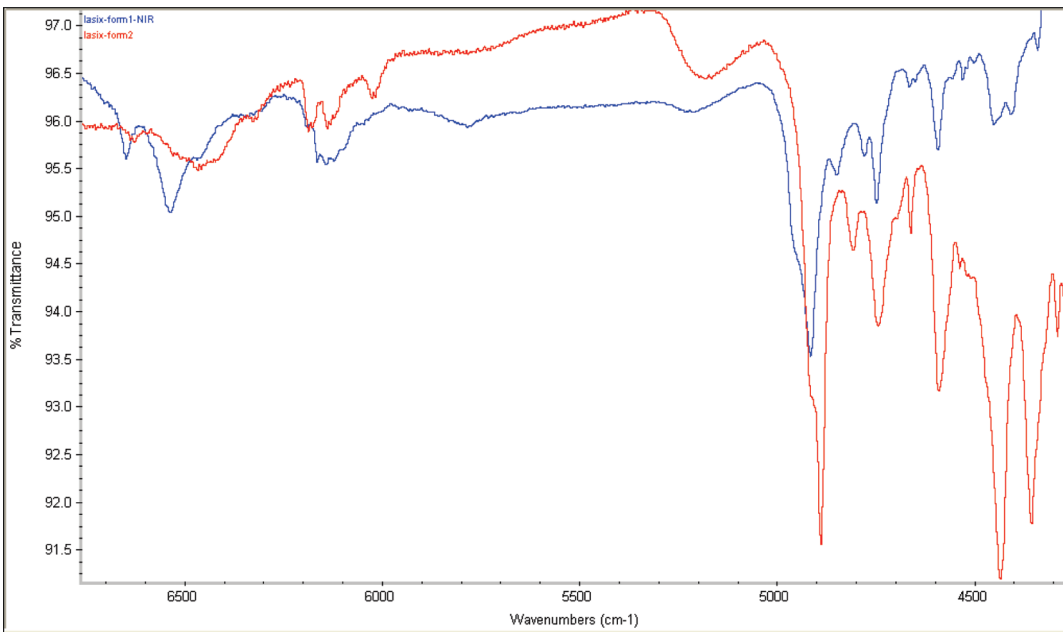


Figure 12. FT-NIR spectra of form 1 (blue) and form 2 (red). Diagnostic IR and NIR peaks are listed in Table S3.

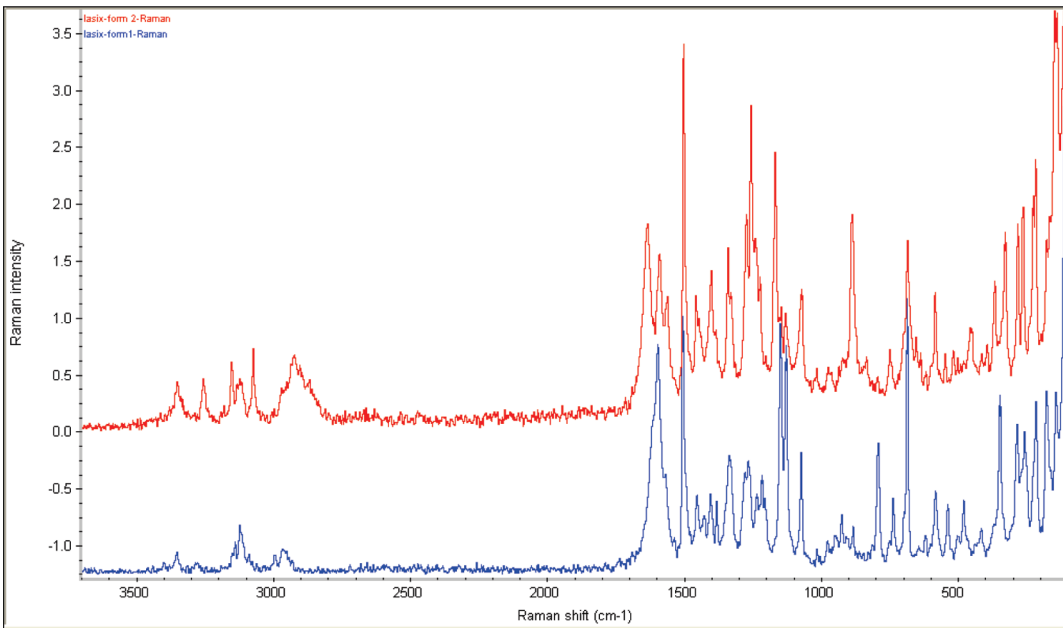


Figure 13. FT-Raman spectra of form 1 (blue) and form 2 (red). Diagnostic Raman peaks are listed in Table S4.

determined in this study correspond to forms III and II of a previous report; form 1 (form I previously) refers to the commercial or reference material.²⁵ Single crystal X-ray diffraction now permits analysis of hydrogen bonding and molecular packing in these polymorphs to quantify their energy and stability relationships.

Phase changes were characterized by X-ray powder diffraction, IR, and Raman spectroscopy. Mechanical grinding of pure furosemide forms 1 or 2 in separate experiments showed no phase conversion. However, when a polymorphic mixture of forms was subjected to grinding in a mortar-pestle phase conversion occurred readily to give form 1 within 1 h. Continued grinding for another 1 h showed complete and quantitative transformation to form 1 by IR spectroscopy (Figure 11), and no evidence of a new phase by XRPD. The

same transformation was accelerated (complete in 15 min) when CH₃CN was used as a lubricant in a solvent-drop grinding method.²⁶ When a polymorphic mixture of forms 1 and 2 was subjected to slurry conversion in CH₃CN, pure form 1 was obtained after 2 d. FT-NIR and Raman spectra of polymorphs 1 and 2 are visibly different for identifying signature peaks (Figures 12 and 13). All these experiments show that polymorph 1 of furosemide is the thermodynamic modification. Crystals of the stable polymorph act as seeds for nucleation of form 1 through a homogeneous (solution) or secondary nucleation (grinding, slurry) pathway.²⁷ The fact that solution crystallization gives pure form 1 from some solvents but concomitant polymorphs from others indicates that their energies are very close, and the concomitant or mixed composition is an intermediate stage of crystallization

when the system has not yet reached the stable polymorph. Further experiments are awaited after we are able to develop a reproducible procedure to prepare a larger quantity of form 3. The very small energy difference of $< 0.5 \text{ kcal mol}^{-1}$ between the stable and metastable polymorphs 1–3 of furosemide and yet the complete transformation to form 1 in stability studies serves as a cautionary note for ranking the most stable polymorph based on lattice energy.²⁸ Moreover, lattice energy of stable form 1 is actually in between those of metastable forms 2 and 3, though by a very small margin. It is clear that the higher crystal density and packing fraction (experimental values from the crystal structure) of form 1 are the primary indicators of its thermodynamic stability. A similar conclusion based on calculated energies for a conformationally flexible molecule with multiple torsions would be almost impossible by structure simulation and energy ranking. The second caution for structure prediction is that the stable crystal structure is derived from a metastable molecular conformation which could not have been anticipated without a prior knowledge of the experimental structure. Thus, once a conformer surface map is generated,²⁹ structure calculations should be carried out not only from those conformers that reside in the global energy minimum but also conformers in metastable minima without bias of conformer energy. The stable crystal structure of furosemide contains molecular conformers which are $\sim 4.5 \text{ kcal mol}^{-1}$ higher in energy than the stable conformation. A third point is that the stable crystal structure has two molecules in the asymmetric unit, whereas most structural chemists and crystallographers would tend to give greater weightage to crystal structures having one molecule in the asymmetric unit,³⁰ in the absence of experimental data.

Conclusions

X-ray crystal structure of only one polymorph of furosemide is reported in the literature even as up to three crystalline modifications have been characterized by XRPD and ss-NMR and vibrational spectroscopy. We report molecular conformation and hydrogen bonding details on X-ray crystal structures of forms 2 and 3 of furosemide, which provide their accurate classification as conformational and synthon polymorphs. Phase transformations show that metastable form 2 converts to form 1 in grinding and slurry crystallization experiments. The stability of thermodynamic form 1 is explained by its more efficient crystal packing and higher density, but the same conclusion could not have been derived from lattice energy calculations. A reproducible procedure for growing crystals of form 3 is still awaited which will provide spectroscopic characterization and phase relationship data for all three polymorphs of furosemide. The thermodynamic polymorph of furosemide form 1 containing two metastable conformers in the crystal structure serves as a reminder that there is no substitute for crystallization experiments and stability testing of drug polymorphs.

Experimental Section

Preparation of Furosemide Polymorphs. Furosemide was extracted from commercial Lasix tablets (Aventis Pharma Ltd.) using methanol solvent. IR and XRPD confirmed the purity of the drug. Crystallization from common solvents such as methanol, ethanol, *n*-propanol, *i*-propanol, acetonitrile invariably yielded furosemide form 1. Very fine needles of form 2 for single crystal X-ray were obtained by slow evaporation of 50 mg of the compound dissolved

in 5 mL of anhydrous MeOH. Form 3 crystals were obtained concomitantly with form 1 when 50 mg of the grinded compound was kept for crystallization in 2 mL acetic acid or 75 mg in 4–5 mL of *n*-propanol.

¹H NMR (DMSO-*d*₆): δ 8.65 (br s, 1H), 8.40 (s, 1H), 7.60 (s, 1H), 7.33 (s, 2H), 7.05 (s, 1H), 6.41 (d, J 4, 1H), 6.35 (d, J 4, 1H), 4.56 (d, J 8, 2H).

X-ray Crystallography. Reflections were collected on Bruker SMART CCD diffractometer. Mo-Kα ($\lambda = 0.71073 \text{ \AA}$) radiation was used to collect X-ray reflections on all crystals (forms 1–3). Data reduction was performed using Bruker SAINT software.³¹ Intensities for absorption were corrected using SADABS.³² Structures were solved and refined using SHELXL-97³³ with anisotropic displacement parameters for non-H atoms. Hydrogen atoms on O and N were experimentally located in all crystal structures. All C–H atoms were fixed geometrically using HFIX command in SHELXTL. RLATT³⁴ was used to visualize *hkl*-reflections for small and big unit cell structures of furosemide form 1. X-Seed³⁵ was used to prepare figures and packing diagrams. A check of the final CIF file using PLATON³⁶ did not show any missed symmetry. Crystallographic parameters for form 1–3 structures are summarized in Table 2. Hydrogen bond distances listed in Table 3 are neutron-normalized to fix D–H distance to its accurate neutron value in X-ray crystal structures (O–H 0.983 Å, N–H 1.009 Å, C–H 1.083 Å). Crystallographic .cif files (CCDC Nos. 761769–761772) are available at www.ccdc.cam.ac.uk/data_request/cif and deposited as Supporting Information.

X-ray Powder Diffraction. Powder XRD of all samples were recorded on a PANalytical 1830 (Philips Analytical) diffractometer using Cu–Kα X-radiation ($\lambda = 1.54056 \text{ \AA}$) at 35 kV and 25 mA. Diffraction patterns were collected over 2θ range of 5–50° at scan rate of 1°/min. Powder Cell 2.3 was used for Rietveld refinement.³⁷

Cambridge Structural Database Searches. The CSD version 5.30, ConQuest 1.11, November 2008 release, Sep 2009 update⁷ was used in all searches and crystal structures were visualized in Mercury 2.2. Only single-component organic crystal structures with *R* < 0.10, no error, and not polymeric were retrieved from the database. The lower *R*-factor structure was retained for duplicate Refcodes. N–H···O distances less than 3.2 Å and angle > 120° are considered.

FT Vibrational Spectroscopy. Nicolet 6700 FT-IR spectrometer with an NXR FT-Raman Module was used to record IR, NIR, and Raman spectra. IR and NIR spectra were recorded on samples dispersed in KBr pellets. Raman spectra were recorded on samples contained in standard NMR diameter tubes or on compressed samples contained in a gold-coated sample holder.

Thermal Analysis. DSC was performed on a Mettler Toledo DSC 822e module. Samples were placed in crimped but vented aluminum sample pans. The typical sample size is 4–6 mg, and the temperature range was 30–250 °C @ 5 K/min. Samples were purged by a stream of dry nitrogen flowing at 150 mL min⁻¹. HSM was performed on a PolythermA Hot Stage and Heitzsch microscope supplied by Wagner & Munz. A Moticam 1000 (1.3 MP) camera supported by software Motic ImagePlus 2.0 ML is used to record images.

Computations. Conformer energies were calculated in Gaussian 03 (B3LYP/6-31G (d,p)).²² Since the observed conformation in the crystal structure is usually different from the gas phase minimized conformer and often higher in energy, constrained optimization of the crystal conformer was carried out by keeping the main torsion angles fixed but allowing bond distances and angles to relax at the nearest local minima (*E*_{conf}). Lattice energies were computed in Cerius² using the COMPASS force field.³⁸ Crystal structures were minimized (*U*_{latt}) by allowing small variations in cell parameters but not gross differences between the calculated and experimental crystal lattice.

Acknowledgment. N.J. and R.T. thank the UGC, and S.C. thanks the ICMR for a research fellowship. We thank the DST for research funding (SR/S1/RFOC-01/2007 and SR/S1/OC-67/2006) and DST (IRPHA) and UGC (PURSE grant) for providing instrumentation and infrastructure facilities.

Supporting Information Available: RLATT, HSM, DSC, XRPD plots, CSD refcodes, spectral peaks, and crystallographic files (.cif)

of furosemide polymorphs are available free of charge via the Internet at <http://pubs.acs.org>.

References

- (1) (a) Friedman, P. A.; Berndt, W. O. In *Modern Pharmacology with Clinical Applications*; 5th ed., Craig, C. R.; Stitzel, R. E., Eds.; Little Brown & Company: Boston, 1997; pp 239–255. (b) Khan, M. G. *Encyclopedia of Heart Diseases*; Elsevier: New York, 2006. (c) <http://en.wikipedia.org/wiki/Furosemide>. (d) <http://www.drugbank.ca/drugs/DB00695>.
- (2) (a) Datta, S.; Grant, D. J. W. *Nat. Rev.* **2004**, *3*, 42. (b) Morissette, S. L.; Souasene, S.; Levinson, D.; Cima, M. J.; Almarsson, Ö. *Proc. Natl. Acad. Sci. U.S.A.* **2003**, *100*, 2180. (c) Almarsson, Ö.; Hickey, M. B.; Peterson, L.; Morissette, S. L.; Soukasene, S.; McNulty, C.; Tawa, M.; MacPhee, J. L.; Remenar, J. F. *J. Cryst. Growth Des.* **2003**, *3*, 927. (d) Byrn, S. R.; Pfeiffer, R. R.; Stowell, J. G. *Solid-State Chemistry of Drugs*; SSCI: West Lafayette, IN, 1999.
- (3) (a) Bernstein, J. *Polymorphism in Molecular Crystals*; Clarendon: Oxford, U. K., 2002. (b) Hilfiker, R., Ed. *Polymorphism in the Pharmaceutical Industry*; Wiley-VCH: Weinheim, Germany, 2006. (c) Matzger, A. J.; Guest Ed. *Special Section on Facets of Polymorphism in Crystals*; *J. Cryst. Growth Des.* **2008**, *8*, 2–161.
- (4) (a) Childs, S. L.; Zaworotko, M. J.; Guest Eds. *Virtual Issue on Pharmaceutical Cocrystals*, *J. Cryst. Growth Des.* **2009**, *9*, 4208. (b) Shan, N.; Zaworotko, M. J. *Drug Disc. Today* **2008**, *13*, 440. (c) Almarsson, Ö.; Zaworotko, M. J. *Chem. Commun.* **2004**, 1889. (d) Morissette, S. L.; Almarsson, Ö.; Peterson, M. L.; Remenar, J. F.; Read, M. J.; Lemmo, A. V.; Ellis, S.; Cima, M. J.; Gardner, C. R. *Adv. Drug Delivery Rev.* **2004**, *56*, 275.
- (5) (a) Doherty, C.; York, P. *Int. J. Pharm.* **1988**, *47*, 141. (b) Matsuda, Y.; Tatsumi, E. *Int. J. Pharm.* **1990**, *60*, 11. (c) Ge, M.; Liu, G.; Ma, S.; Wang, W. *Bull. Korean Chem. Soc.* **2009**, *30*, 2265.
- (6) (a) Fronckowiak, M.; Hauptman, H. *ACA Abstr. Papers (Winter)* **1976**, *9* (CSD refcode FURSEM). (b) Lamotte, J.; Campsteyn, H.; Dupont, L.; Vermeire, M. *Acta Crystallogr.* **1978**, *B34*, 689 (FURSEM01). (c) Shin, W.; Jeon, G. S. *Cha. Kwa. Tae. Nom. (Seoul Tae.) (Kor.) (Proc. Coll. Nat. Sci., SNU)* **1983**, *8*, 45 (FURSEM02). (d) Sarojini, B. K.; Yathirajan, H. S.; Narayana, B.; Sunil, K.; Bolte, M. *Private Communication* **2007**, CCDC No. 657920 (FURSEM03). (e) Preliminary crystallographic results were presented in a poster abstract. Babu, N. J.; Nangia, A. *Acta Crystallogr.* **2008**, *A64*, C449.
- (7) Cambridge Structural Database, ver. 5.30, ConQuest 1.11, November 2008 release, Sep 2009 update; www.ccdc.cam.ac.uk.
- (8) Karami, S.; Li, Y.; Hughes, D. S.; Hursthouse, M. B.; Russell, A. E.; Threlfall, T. L.; Claybourn, M.; Roberts, R. *Acta Crystallogr.* **2006**, *B62*, 689.
- (9) (a) Corradini, P. *Chem. Ind. (Milan)* **1973**, *55*, 122. (b) Bernstein, J. Conformational Polymorphism. In *Organic Solid State Chemistry*; Desiraju, G. R., Ed.; Elsevier: Amsterdam, 1987, pp. 471–518.
- (10) Vippagunta, S. R.; Brittain, H. G.; Grant, D. J. W. *Adv. Drug Delivery Rev.* **2001**, *48*, 3.
- (11) (a) Thun, J.; Seyfarth, L.; Butterhof, C.; Senker, J.; Dinnebier, R. E.; Breu, J. *J. Cryst. Growth Des.* **2009**, *9*, 2435. (b) Blagden, N.; Davey, R.; Dent, G.; Song, M.; David, W. I. F.; Pulham, C. R.; Shankland, K. *J. Cryst. Growth Des.* **2005**, *5*, 2218.
- (12) (a) Grzesiak, A. L.; Lang, M.; Kim, K.; Matzger, A. J. *J. Pharm. Sci.* **2003**, *92*, 2260. (b) Rodríguez-Spong, B.; Price, C. P.; Jayasankar, A.; Matzger, A. J.; Rodríguez-Hornedo, N. *Adv. Drug Delivery Rev.* **2004**, *56*, 241.
- (13) Nangia, A. *Acc. Chem. Res.* **2008**, *41*, 595.
- (14) (a) Bauer, J.; Spanton, S.; Henry, R.; Quick, J.; Dziki, W.; Porter, W.; Morris, J. *Pharm. Res.* **2001**, *18*, 856. (b) Chemburkar, S. R.; Bauer, J.; Deming, K.; Spiwek, H.; Patel, K.; Morris, J.; Henry, R.; Spanton, S.; Dziki, W.; Porter, W.; Quick, J.; Bauer, P.; Donaubauer, J.; Narayanan, B. A.; Soldani, M.; Riley, D.; McFarland, K. *Org. Process Res. Dev.* **2000**, *4*, 413.
- (15) (a) Andersen, K. V.; Larsen, S.; Alhede, B.; Gelting, N.; Buchardt, O. *J. Chem. Soc., Perkin Trans. 2* **1989**, 1443. (b) López-Mejías, V.; Kampf, J. W.; Matzger, A. J. *J. Am. Chem. Soc.* **2009**, *131*, 4554.
- (16) (a) Yu, L.; Stephenson, G. A.; Mitchell, C. A.; Bunnell, C. A.; Snorek, S. V.; Bowyer, J. J.; Borchardt, T. B.; Stowell, J. G.; Byrn, S. R. *J. Am. Chem. Soc.* **2000**, *122*, 585. (b) Chen, S.; Guzei, I. A.; Yu, L. *J. Am. Chem. Soc.* **2005**, *127*, 9881.
- (17) (a) Jetti, R. K. R.; Boese, R.; Sarma, J. A. R. P.; Reddy, L. S.; Vishweshwar, P.; Desiraju, G. R. *Angew. Chem., Int. Ed.* **2003**, *42*, 1963. (b) Sreekanth, B. R.; Vishweshwar, P.; Vyas, K. *Chem. Commun.* **2007**, 2375.
- (18) (a) Derissen, J. L.; Smit, P. H. *Acta Crystallogr.* **1974**, *B30*, 2240. (b) Benghiat, V.; Leiserowitz, L. *J. Chem. Soc., Perkin Trans. 2* **1972**, 1763. (c) Parveen, S.; Davey, R. J.; Dent, G.; Pritchard, R. G. *Chem. Commun.* **2005**, 1531. (d) Gavezzotti, A.; Filippini, G.; Kroon, J.; van Eijck, B. P.; Klewinghaus, P. *Chem.—Eur. J.* **1997**, *3*, 894.
- (19) (a) Lowe, P. R.; Sansom, C. E.; Schwalbe, C. H.; Stevens, M. F. G.; Clark, A. S. *J. Med. Chem.* **1992**, *35*, 3377. (b) Babu, N. J.; Reddy, L. S.; Aitipamula, S.; Nangia, A. *Chem. Asian J.* **2008**, *3*, 1122.
- (20) (a) Gelbrich, T.; Hughes, D. S.; Hursthouse, M. B.; Threlfall, T. L. *CrystEngComm* **2008**, *10*, 1328. (b) Kruger, G. J.; Gafner, G. *Acta Crystallogr.* **1971**, *B27*, 326. (c) Kruger, G. J.; Gafner, G. *Acta Crystallogr.* **1972**, *B28*, 272.
- (21) (a) Etter, M. C.; MacDonald, J. C.; Bernstein, J. *Acta Crystallogr.* **1990**, *B46*, 256. (b) Bernstein, J.; Davis, R. E.; Shimoni, L.; Chang, N.-L. *Angew. Chem., Int. Ed.* **1995**, *34*, 1555.
- (22) Gaussian 03, Revision B.05, www.gaussian.com.
- (23) (a) McKinnon, J. J.; Spackman, M. A.; Mitchell, A. S. *Acta Crystallogr.* **2004**, *B60*, 627. (b) Spackman, M. A.; Jayatilaka, D. *CrystEngComm* **2009**, *11*, 19. (c) McKinnon, J. J.; Jayatilaka, D.; Spackman, M. A. *Chem. Commun.* **2007**, 3814.
- (24) Burger, A.; Ramberger, R. *Mikrochim. Acta II* **1979**, *II*, 273.
- (25) The numbering of forms 1, 2, and 3 in this paper is based on the chronological order in which they were originally characterized by XRPD (ref 5a and 5b).
- (26) (a) Trask, A. V.; Shan, N.; Motherwell, W. D. S.; Jones, W.; Feng, S.; Tan, R. B. H.; Carpenter, K. *J. Chem. Commun.* **2005**, 880. (b) Trask, A. V.; Jones, W. *Top. Curr. Chem.* **2005**, 254, 41.
- (27) (a) Bernstein, J.; Davey, R. J.; Henk, J. *Angew. Chem., Int. Ed.* **1999**, *38*, 3440. (b) Davey, R. J.; Blagden, N.; Righini, S.; Alison, H.; Ferrari, E. S. *J. Phys. Chem. B* **2002**, *106*, 1954.
- (28) Motherwell, W. D. S.; Ammon, H. L.; Dunitz, J. D.; Dzyabchenko, A.; Erk, P.; Gavezzotti, A.; Hofmann, D. W. M.; Leusen, F. J. J.; Lommersse, J. P. M.; Mooij, W. T. M.; Price, S. L.; Scheraga, H.; Schweizer, B.; Schmidt, M. U.; van Eijck, B. P.; Verwer, P.; Williams, D. E. *Acta Crystallogr.* **2002**, *B58*, 647. (b) Jetti, R. K. R.; Boese, R.; Sharma, J. A. R. P.; Reddy, L. S.; Vishweshwar, P.; Desiraju, G. R. *Angew. Chem., Int. Ed.* **2003**, *42*, 1963. (c) Roy, S.; Matzger, A. J. *Angew. Chem., Int. Ed.* **2009**, *48*, 8505.
- (29) (a) Lewis, T. C.; Tocher, D. A.; Price, S. L. *J. Cryst. Growth Des.* **2004**, *4*, 979. (b) Ouvard, C.; Price, S. L. *J. Cryst. Growth Des.* **2004**, *4*, 1119. (c) Nowell, H.; Price, S. L. *Acta Crystallogr.* **2005**, *B61*, 558. (d) Johnston, A.; Florence, A. J.; Shankland, N.; Kennedy, A. R.; Shankland, K.; Price, S. L. *J. Cryst. Growth Des.* **2007**, *7*, 705.
- (30) In a polymorph set, the high Z' crystal structure is generally considered to be a metastable form on way to the more stable modification ($Z' = 1$). (a) Das, D.; Banerjee, R.; Mondal, R.; Howard, J. A. K.; Boese, R.; Desiraju, G. R. *Chem. Commun.* **2006**, 555. (b) Roy, S.; Banerjee, R.; Nangia, A.; Kruger, G. J. *Chem.—Eur. J.* **2006**, *12*, 3777. (c) Steed, J. W. *CrystEngComm* **2003**, *5*, 169. However, exceptions are known when the high Z' structure is the stable polymorph. (d) Roy, S.; Bhatt, P. M.; Nangia, A.; Kruger, G. J. *J. Cryst. Growth Des.* **2007**, *7*, 476.
- (31) SAINT-Plus, version 6.45; Bruker AXS Inc.: Madison, WI, 2003.
- (32) Sheldrick, G. M., SADABS, *Program for Empirical Absorption Correction of Area Detector Data*, University of Göttingen, Germany, 1997.
- (33) (a) SMART (Version 5.625) and SHELX-TL (Version 6.12); Bruker AXS Inc.: Madison, WI, 2000. (b) Sheldrick, G. M. *SHELXS-97 and SHELXL-97*; University of Göttingen, Germany, 1997.
- (34) RLATT (reciprocal lattice display program); Bruker AXS Inc.: Madison, WI, 1998.
- (35) Barbour, L. J. *X-Seed, Graphical Interface to SHELX-97 and POV-Ray*, University of Missouri-Columbia, USA, 1999.
- (36) Spek, A. L. PLATON, *A Multipurpose Crystallographic Tool*; Utrecht University: Utrecht, Netherland, 2002. Spek, A. L. *J. Appl. Crystallogr.* **2003**, *36*, 7.
- (37) Powder Cell for structure visualization, powder pattern calculation and profile fitting, www.ccp14.ac.uk.
- (38) Cerius², Ver. 4, www.accelrys.com.